NeuroImage: Clinical 45 (2025) 103726

Contents lists available at ScienceDirect

NeuroImage: Clinical

journal homepage: www.elsevier.com/locate/ynicl

Consistent frontal-limbic-occipital connections in distinguishing treatment-resistant and non-treatment-resistant schizophrenia

Yijie Zhang [a,b,1], Shuzhan Gao [c,1], Chuang Liang [a,b], Juan Bustillo [d], Peter Kochunov [e], Jessica A. Turner [f], Vince D. Calhoun [f], Lei Wu [f], Zening Fu [f], Rongtao Jiang [g], Daoqiang Zhang [a,b], Jing Jiang [c], Fan Wu [c], Ting Peng [c], Xijia Xu [c,*], Shile Qi [a,b,*]

[a] College of Artificial Intelligence, Nanjing University of Aeronautics and Astronautics, Nanjing, China
[b] The Key Laboratory of Brain-Machine Intelligence Technology, Ministry of Education, Nanjing University of Aeronautics and Astronautics, Nanjing, China
[c] Department of Psychiatry, the Affiliated Brain Hospital of Nanjing Medical University, Nanjing, China
[d] Departments of Neurosciences and Psychiatry and Behavioral Sciences, University of New Mexico, Albuquerque, NM, USA
[e] Department of Psychiatry and Behavioral Sciences, University of Texas Health Science Center Houston, Houston, TX, USA
[f] Tri-institutional Center for Translational Research in Neuroimaging and Data Science (TReNDS) Georgia State University, Georgia Institute of Technology, Emory University, Atlanta, GA, USA
[g] Department of Radiology and Biomedical Imaging, Yale University, New Haven, CT, USA

ARTICLE INFO

Keywords:
Treatment-resistant schizophrenia
Resting-state fMRI
Functional connection
Brain atlas
Machine learning
Brain network

ABSTRACT

Background and hypothesis: Treatment-resistant schizophrenia (TR-SZ) and non-treatment-resistant schizophrenia (NTR-SZ) lack specific biomarkers to distinguish from each other. This investigation aims to identify consistent dysfunctional brain connections with different atlases, multiple feature selection strategies, and several classifiers in distinguishing TR-SZ and NTR-SZ.

Study design: 55 TR-SZs, 239 NTR-SZs, and 87 healthy controls (HCs) were recruited from the Affiliated Brain Hospital of Nanjing Medical University. Resting-state functional connection (FC) matrices were constructed from automated anatomical labeling (AAL), Yeo-Networks (YEO) and Brainnetome (BNA) atlases. Two feature selection methods (Select From Model and Recursive Feature Elimination) and four classifiers (Adaptive Boost, Bernoulli Naïve Bayes, Gradient Boosting and Random Forest) were combined to identify the consistent FCs in distinguishing TR-SZ and HC, NTR-SZ and HC, TR-SZ and NTR-SZ.

Study results: The whole brain FCs, except the temporal-occipital FC, were consistent in distinguishing SZ and HC. Abnormal frontal-limbic, frontal-parietal and occipital-temporal FCs were consistent in distinguishing TR-SZ and NTR-SZ, that were further correlated with disease progression, symptoms and medication dosage. Moreover, the frontal-limbic and frontal-parietal FCs were highly consistent for the diagnosis of SZ (TR-SZ vs. HC, NTR-SZ vs. HC and TR-SZ vs. NTR-SZ). The BNA atlas achieved the highest classification accuracy (>90 %) comparing with AAL and YEO in the most diagnostic tasks.

Conclusions: These results indicate that the frontal-limbic and the frontal-parietal FCs are the robust neural pathways in the diagnosis of SZ, whereas the frontal-limbic, frontal-parietal and occipital-temporal FCs may be informative in recognizing those TR-SZ in the clinical practice.

1. Introduction

Schizophrenia (SZ) is a severe, chronic and debilitating mental illness, characterized by positive and negative symptoms, and cognitive deficits (Qi et al., 2020), with a clinical burden compounded by high rate (Correll et al., 2022; Siskind et al., 2022) (up to 30%) of non-responders to modern medications, a condition which is defined as treatment-resistant schizophrenia (TR-SZ). Compared to non-TR-SZ (NTR-SZ), TR-SZ exhibits an higher genetic and environmental risks (Crespo-Facorro et al., 2013), earlier age of onset, lower rates of functional

* Corresponding authors at: The Affiliated Brain Hospital of Nanjing Medical University, Nanjing, China (X. Xu); College of Artificial Intelligence, Nanjing University of Aeronautics and Astronautics, Nanjing, China (S. Qi).
E-mail addresses: xuxijia@c-nbh.com (X. Xu), shile.qi@nuaa.edu.cn (S. Qi).
[1] Contributed equally to this work.

https://doi.org/10.1016/j.nicl.2024.103726
Received 9 August 2024; Received in revised form 10 December 2024; Accepted 11 December 2024
Available online 12 December 2024

recovery and higher overall clinical burden (Nucifora et al., 2019). Furthermore, existing studies suggest that TR−SZ may be a more familial form of SZ (Crespo-Facorro et al., 2013) and that TR-SZ and NTR-SZ probably originate from different pathophysiological mechanisms (Shin et al., 2022), reflected in different brain changes (Nucifora et al., 2019), indicating that TR-SZ may be a distinct subtype of SZ. Thus, identifying such differences may have diagnostic value for TR-SZ, such as distinguishing patients who are likely to fail antipsychotic treatment and whom may need earlier intervention with clozapine (the only drug established for TR-SZ).

Numerous neuroimaging-based studies have reported brain structural and functional differences between TR-SZ and NTR-SZ. Reduced frontal and temporal cortical thickness in TR-SZ comparing with NTR-SZ/healthy control (HC) was reported as the most consistent findings in structural magnetic resonance imaging (sMRI)-based studies (Barry et al., 2019; Itahashi et al., 2021; Shah et al., 2020; Wannan et al., 2019; Zugman et al., 2013). Furthermore, lower fractional anisotropy in the superior longitudinal fasciculus (Aggarwal et al., 2021; Matrone et al., 2022; McNabb et al., 2020; Ochi et al., 2020) was identified in multiple diffusion MRI (dMRI) studies of TR-SZ. Functional MRI (fMRI) provides intricate information on the connectivity among brain regions and therefore may present a more sensitive TR biomarker comparing with structural imaging. One previous study observed no difference in the whole-brain connectivity between HC and SZ, including NTR-SZ and TR-SZ (McNabb et al., 2018). Other studies found both decreased whole-brain functional connections (FCs) (Ganella et al., 2017) and reduced frontal-temporal-occipital FCs in TR-SZ (Ganella et al., 2017). Differences within thalamic subregions and medial frontal cortex FC were observed between TR-SZ and HC (Kim et al., 2022). However, there is no consistent functional neuroimaging biomarkers that reflects the differences between TR-SZ and NTR-SZ. The focus of this study is to identify the consistent FC biomarkers that could distinguish TR-SZ and NTR-SZ.

Due to its noninvasiveness and high spatial and relatively high temporal resolution, fMRI is a natural choice for investigating the brain network dysfunction in brain disorders (Canario et al., 2021; Finn et al., 2023). Several FC-based studies have attempted to develop biomarkers sensitive to SZ. A study constructing FC matrix based on a multiscale functional template (64 regions) atlas found that the whole brain FCs contributed to the distinction between SZ and HC when using a support vector machine (SVM) classifier (Orban et al., 2018). The same SVM using an automated anatomical labeling (AAL) atlas showed decreased strength in anterior right cingulate cortex, inferior left parietal cortex and superior right temporal cortex has been identified as diagnostic features for SZ (Bae et al., 2018). Kendall tau rank correlation coefficient downscaling strategy indicate that the visual network is crucial for the diagnosis of SZ (Su et al., 2013). However, the selected false discovery rate (SelectFdr) of scikit-learn feature selection strategy highlighted that frontal-limbic regions show the potential for SZ and HC classification (Liang et al., 2020). A 3-dimensional convolutional neural network (3D-CNN) classification framework identified the visual network and the central executive network as the most discriminating features between SZ and HC (Qureshi et al., 2019), while through recurrent neural network (RNN), the distinguishing features was located at inferior frontal gyrus, putamen, lentiform nucleus, parahippocampal gyrus and caudate (Yan et al., 2019). Collectively, current fMRI-based SZ diagnostic studies are inconsistent likely due to the exiting numerous brain atlases (Moghimi et al., 2022), feature selection strategies, classifiers, limited sample size ($\leq$ 50). Previous studies reported classification accuracies for differentiating SZ from HC ranging from 0.72 to 0.92 (Bae et al., 2018; Itahashi et al., 2021; Liang et al., 2023; Liang et al., 2020; Orban et al., 2018; Qi et al., 2022; Shi et al., 2021; Winterburn et al., 2019; Yan et al., 2019; Zhao et al., 2024). These variations could be biased due to methodological inconsistencies, which leads to differences in classification performance across studies. Such biases could compromise the validity of these results as accurate representations of the genuine underlying neural mechanisms associated with SZ diagnosis. Therefore, it is crucial to identify consistent and robust FCs for the diagnosis of TR-SZ across multiple atlases, feature selection strategies, classifiers and under larger samples (Elliott et al., 2021), while ensuring high accuracy.

In the present study, we aim to identify consistent and robust resting-state brain FCs in distinguishing TR-SZ and HC, NTR-SZ and HC, as well as TR-SZ and NTR-SZ over three commonly used brain atlases (including AAL (Tzourio-mazoyer et al., 2002); Yeo-Networks (Tian et al., 2020; Yeo et al., 2011), YEO; and Brainnetome (Fan et al., 2016), BNA) by combing two dimensionality reduction methods (Select From Model, SFM; Recursive Feature Elimination, RFE) with four classifiers (Adaptive Boost (Schapire, 2013), Adaboost; Bernoulli Naïve Bayes (Dai et al., 2013; Rish, 2001), Gradient Boosting (Natekin and Knoll, 2013) and Random Forest (Breiman, 2001)). The AAL and BNA are representative structural brain atlases, while YEO is a functional brain parcellation. SFM and RFE are the two classical feature selection methods that adopt different strategies and criteria in evaluating features. Adaptive boost, Bernoulli Naïve Bayes, Gradient Boosting and Random Forest are the representative classifiers that were commonly used in the diagnosis of patients. By employing diverse methodologies, including the use of multiple brain atlases, dimensionality reduction techniques, and classifiers, we validate the robustness of our research findings. This redundancy strategy enhances the credibility and generalizability of our conclusions, demonstrating consistency across different conditions and minimizing the likelihood of chance or bias.

2. Methods and materials

2.1. Participants

A total of 381 subjects, including 55 TR-SZs, 239 NTR-SZs, and 87 HCs were consecutively recruited from the Affiliated Brain Hospital of Nanjing Medical University. Diagnosis of SZ was confirmed by two experienced psychiatrists with the position of associate chief physician or higher using the Structured Clinical Interview according to the World Health Organization's International Classification of Diseases (ICD)-10 (WHO, 1992). The severity of SZ symptoms was assessed with the Positive and Negative Syndrome Scale (PANSS) (Kay et al., 1987). For the TR-SZ, the criteria for enrollment are as follows: (1) Absence of significant improvement in psychopathology or other target symptoms, despite undergoing treatment with two different antipsychotics from at least two distinct chemical classes over the past five years; At least one of these medications should be an atypical antipsychotic; Treatment should have been administered at recommended dosages for a duration of 2 to 8 weeks per drug; Absence of significant improvement was defined as reduction rate of total PANSS<20% (Hasan et al., 2012); (2) Resistant positive symptoms required that at least two positive symptom items have scores of 4 or higher, or one positive symptom item has a score of 5 or higher in PANSS assessment (Howes et al., 2017). For the NTR-SZ, the criteria for enrollment are as follows: (1) Failure to meet the criteria for TR-SZ (Hasan et al., 2012); (2) Reduction rate of total PANSS>20% (Howes et al., 2017). Treatment doses of different types of antipsychotic drugs are converted to equivalent doses of olanzapine (OLA-ED) (Leucht et al., 2016).

The exclusion criteria for patients were as follows: (1) Organic mental disorders, psychoactive substances abuse, intellectual disability (IQ < 70), mood disorders, mental disorders resulting from physical illness, (2) Known central nervous system diseases, such as encephalitis, epilepsy, brain trauma, and severe physical illnesses, (3) Contraindications for MRI scanning, including pregnancy or presence of metal foreign bodies, (4) Patients who had undergone electroconvulsive therapy within the past 6 months. Exclusion criteria for HCs were as follows: (1) Presence of mental illness, (2) Family history of mental illness, (3) Previous use of antipsychotic medication, (4) Organic mental disorders, psychoactive substances abuse, intellectual disability (IQ < 70), mood disorders, mental disorders resulting from physical illness, (5)

Known central nervous system diseases, such as encephalitis, epilepsy, brain trauma, and severe physical illnesses, (6) Contraindications for MRI scanning, including pregnancy or presence of metal foreign bodies, (7) Patients who had undergone electroconvulsive therapy within the past 6 months.

Participants were informed about the study procedures. Written informed consent was obtained from all participants and their legal guardians. The study was approved by the local Ethics Committee of the Affiliated Nanjing Brain Hospital, Nanjing Medical University (No. KY44, 2011). The demographic and clinical information are summarized in Table 1. Details on the scanning parameters and preprocessing steps can be found in Supplementary "Imaging parameters and preprocessing".

3. Study design

Based on the analytic plan pointed out in the introduction, we conducted the following procedures. FC matrices were constructed from AAL (90 regions of interest, ROIs; Supplementary Table 1; (Tzourio-mazoyer et al., 2002)), YEO (130 ROIs; Supplementary Table 2; (Tian et al., 2020; Yeo et al., 2011)), BNA (246 ROIs; Supplementary Table 3; (Fan et al., 2016)) atlases separately, by calculating the Pearson correlation of the mean time series for each pair of brain regions (Fig. 1a). The lower triangle of the FC matrices was flattened to obtain the feature matrix (subjects × $\frac{ROIs\times(ROIs-1)}{2}$). FMRI data retrieval, FC matrix construction, feature selection and classifications were all conducted on the PyCharm platform. Two feature selection approaches (SFM and RFE) with four classifiers (Adaptive Boost, Bernoulli naïve Bayes, Gradient Boosting and Random Forest) were combined to classify between TR-SZ and HC, NTR-SZ and HC, as well as TR-SZ and NTR-SZ (Fig. 1b). 1000 features were selected by SFM or RFE among $\frac{ROIs\times(ROIs-1)}{2}$ features within each fold during cross-validation in the following classifications. Prior to each 5-fold cross-validation, a data balancing operation was performed. The unbalanced NTR-SZ data were randomly subsampled to match the amount of TR-SZ. Subsequently, the balanced dataset was then divided randomly and equally into five parts. Four of these parts were used as training set to fit the model, while the remaining part was used as a test set to verify the model's accuracy. This process was repeated 1000 times. The top 40% contributed FCs under 1000 times 5-fold cross-validation were used to find the most consistent FCs across the 3 brain atlases (Fig. 1**c**), over 2 feature selection (SFM and RFE) and 4 classification methods (Adaboost, Bernoulli Naïve Bayes, Gradient Boosting and Random Forest). SFM and RFE could extract the contributed FCs directly without altering the original features. The four traditional classifiers are universally applicable and have the potential to identify more robust FCs. The above mentioned, including fMRI data retrieval, FC matrix construction, feature selection and classification, were all conducted on the PyCharm platform, along with third-party libraries such as 'sklearn', using the Python language for programming. Supplementary Table 4 provides details on the functions used and their specific parameters. Age, gender and education (Table 1) were regressed out prior to the classification analysis.

4. Results

4.1. Classification results

The classification accuracy in distinguishing between TR-SZ and HC, NTR-SZ and HC, as well as TR-SZ and NTR-SZ were displayed in Supplementary Fig. 1. For the three diagnostic tasks, the mean ± standard deviation classification accuracies of the 24 combinations under 1000 times 5-fold cross-validation were as follows: TR-SZ vs. HC: 0.90 ± 0.05, NTR-SZ vs. HC: 0.80 ± 0.04 and TR-SZ vs. NTR-SZ: 0.74 ± 0.04, respectively. The BNA, RFE combined with Bernoulli classifiers produced the optimum results for all the diagnostic tasks (TR-SZ vs. HC: 0.99, NTR-SZ vs. HC: 0.98 and TR-SZ vs. NTR-SZ: 0.92).

4.2. Consistent FCs in distinguish TR-SZ and HC

The FCs between inferior frontal gyrus-superior temporal gyrus/supramarginal gyrus, precental gyrus-inferior temporal gyrus/rolandic operculum, superior parietal gyrus-inferior occipital gyrus/hippocampus/parahippocampal gyrus, inferior parietal gyrus-insula, cuneus-middle frontal gyrus/postcentral gyrus/inferior parietal gyrus/supramarginal gyrus, precuneus-superior temporal gyrus/hippocampus/angular gyrus, angular gyrus-heschl gyrus, amygdala-superior frontal gyrus/rolandic operculum and putamen-olfactory cortex/supramarginal gyrus were the consistent FCs among 2 feature selections and 4 classifiers for AAL (Fig. 2**a**). The FCs between control network-default mode network/somatomotor/dorsal attention network, visual-dorsal attention network, ventral attention network-default mode network/somatomotor/ventral attention network/subcortex and subcortex-visual network/limbic/somatomotor/subcortex were the consistent for YEO (Fig. 2**b**). The FCs between superior frontal gyrus-precentral gyrus/basal ganglia/thalamus, middle frontal gyrus-superior temporal gyrus/inferior temporal gyrus, precuneus-precentral gyrus/superior temporal

Table 1
Demographic and clinical information of TR-SZ, NTR-SZ and HC.

		TR-SZ	NTR-SZ	HC	$p1$[a]	$p2$[b]	$p3$[c]	$p4$[d]
Demographic characteristics								
Sample size (N)		N = 55	N = 239	N = 87				
Age (year)		36.1 ± 11	31.9 ± 10.1	29.5 ± 7.1	0.011	1.6×10^{-4}	0.02	0.002
Gender (M/F)		23/32	64/175	41/46	0.043	0.54	0.0011	2.3×10^{-4}
Education (year)		12.3 ± 2.6	13.2 ± 3.7	15.3 ± 2.7	0.048	1.3×10^{-9}	2.6×10^{-8}	3.3×10^{-8}
Clinical characteristics								
Onset (year)		19.1 ± 4.3	26.7 ± 9.0	n/a	7.9×10^{-17}	n/a	n/a	n/a
Duration (year)		17.1 ± 9.4	5.4 ± 5.4	n/a	8.3×10^{-13}	n/a	n/a	n/a
OLA-ED (mg/day)		15.0 ± 7.6	10.7 ± 17.1	n/a	0.0048	n/a	n/a	n/a
PANSS	Positive	26.7 ± 5.0	23.2 ± 6.5	n/a	2.8×10^{-5}	n/a	n/a	n/a
	Negative	22.2 ± 5.7	19.9 ± 7.6	n/a	0.016	n/a	n/a	n/a
	General	46.7 ± 7.2	40.6 ± 9.0	n/a	3.8×10^{-7}	n/a	n/a	n/a
	Total	95.6 ± 14.3	83.7 ± 19.5	n/a	1.2×10^{-6}	n/a	n/a	n/a

Abbreviations: (alphabetical order)**: HC:** healthy control, **NTR-SZ:** non-treatment-resistant schizophrenia, **OLA-ED:** equivalent doses of olanzapine, **PANSS:** Positive and Negative Syndrome Scale, **TR-SZ:** treatment-resistant schizophrenia.

a. "*p1*" denotes the p values for the correlation between TR-SZ and NTR-SZ.
b. "*p2*" denotes the p values for the correlation between TR-SZ and HC.
c. "*p3*" denotes the p values for the correlation between NTR-SZ and HC.
d. "*p4*" denotes the p values for the correlation between TR-SZ, NTR-SZ and HC.
A ± B represents mean ± standard deviation

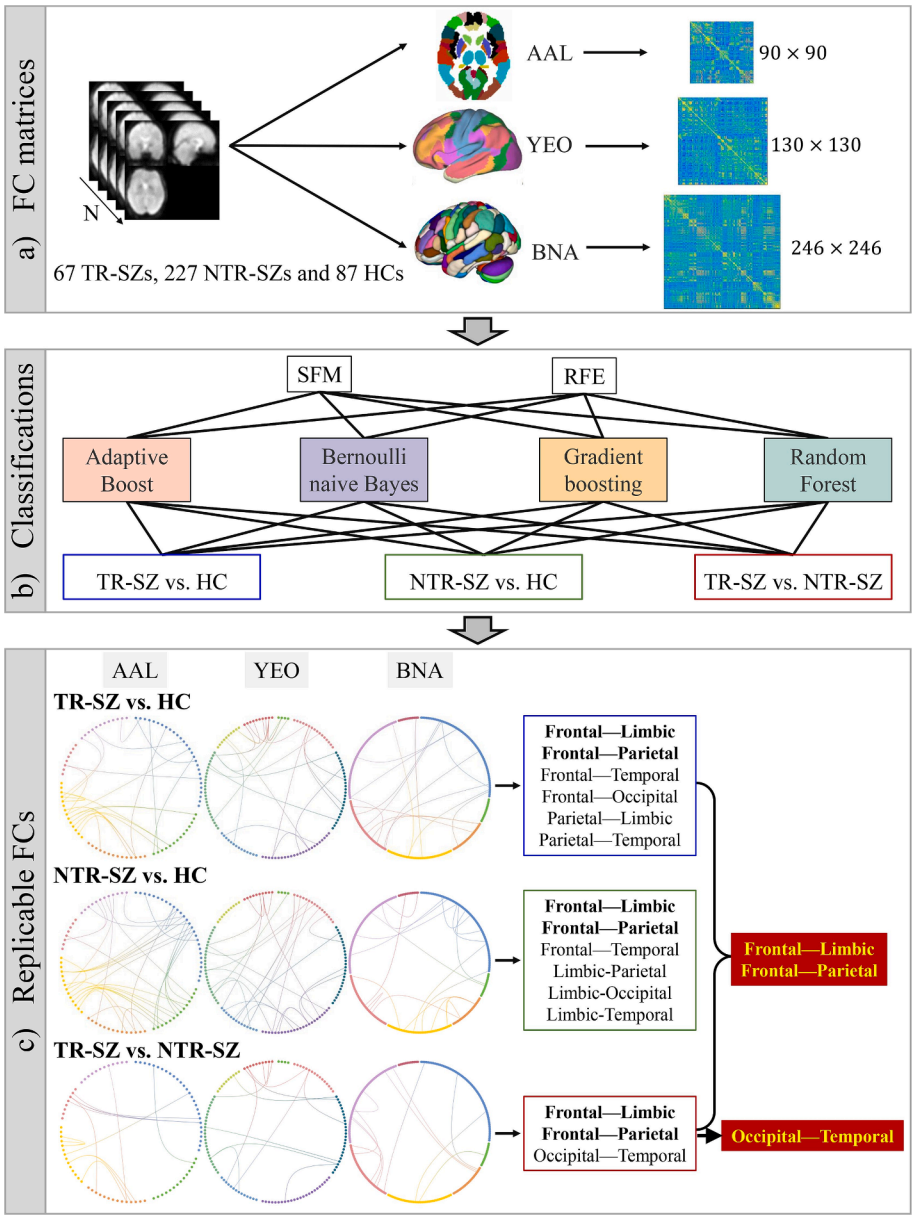

Fig. 1. The workflow of this study. (a) FC matrices construction over 3 atlases. (b) Classification between TR-SZ and HC, NTR-SZ and HC, as well as TR-SZ and NTR-SZ with 2 feature selection methods and 4 classifiers. (c) Consistent FCs across the 3 atlases, 2 feature selections and 4 classifiers. Abbreviations (alphabetical order): AAL: automated anatomical labeling, BNA: Brainnetome, FC: Functional connection, HC: healthy control, NTR-SZ: non-treatment-resistant schizophrenia, RFE: Recursive Feature Elimination, SFM: Select From Model, TR-SZ: treatment-resistant schizophrenia, YEO: Yeo-Networks.

sulcus, amygdala-orbital gyrus/precentral gyrus, medial occipital cortex-basal ganglia/thalamus, inferior parietal lobule-insular gyrus, paracentral lobule-lateral occipital cortex, superior temporal gyrus-hippocampus were the consistent for BNA (Fig. 2**c**). Details on the consistent FCs over AAL, YEO and BNA in distinguishing TR-SZ and HC can be found in Supplementary Table 5**.** Comparing AAL, YEO and BNA, the frontal-limbic, frontal-parietal, frontal-temporal, frontal-occipital, parietal-limbic and parietal-temporal FCs were consistent in distinguish TR-SZ and HC.

4.3. Consistent FCs in distinguish NTR-SZ and HC

The FCs between inferior frontal gyrus-middle frontal gyrus/anterior cingulate gyri/posterior cingulate gyrus/amygdala/supramarginal gyrus/precuneus/superior temporal gyrus/inferior temporal gyrus, postcentral gyrus-lingual gyrus/rolandic operculum, superior parietal gyrus-hippocampus/parahippocampal gyrus, cuneus-middle frontal gyrus/supramarginal gyrus, inferior parietal gyrus-median cingulate gyri/posterior cingulate gyrus/paracentral lobule, putamen-median cingulate gyri/superior temporal gyrus, amygdala-rolandic operculum/lingual gyrus, middle temporal gyrus-anterior cingulate gyri/inferior occipital gyrus/supramarginal gyrus, calcarine fissure-fusiform gyrus were the consistent for AAL (Fig. 3**a**). The FCs between control network-default mode network/dorsal attention network/somatomotor/subcortex, default mode network-ventral attention network/limbic, visual network-ventral attention network/visual, subcortex-somatomotor/ventral attention network/subcortex, ventral attention network-ventral attention network were the consistent for YEO (Fig. 3**b**). The FCs between middle frontal gyrus-orbital gyrus/superior temporal gyrus/inferior temporal gyrus/parahippocampal gyrus, inferior frontal gyrus-superior frontal gyrus/orbital gyrus, medial occipital cortex-superior parietal lobule/inferior parietal lobule, insular-

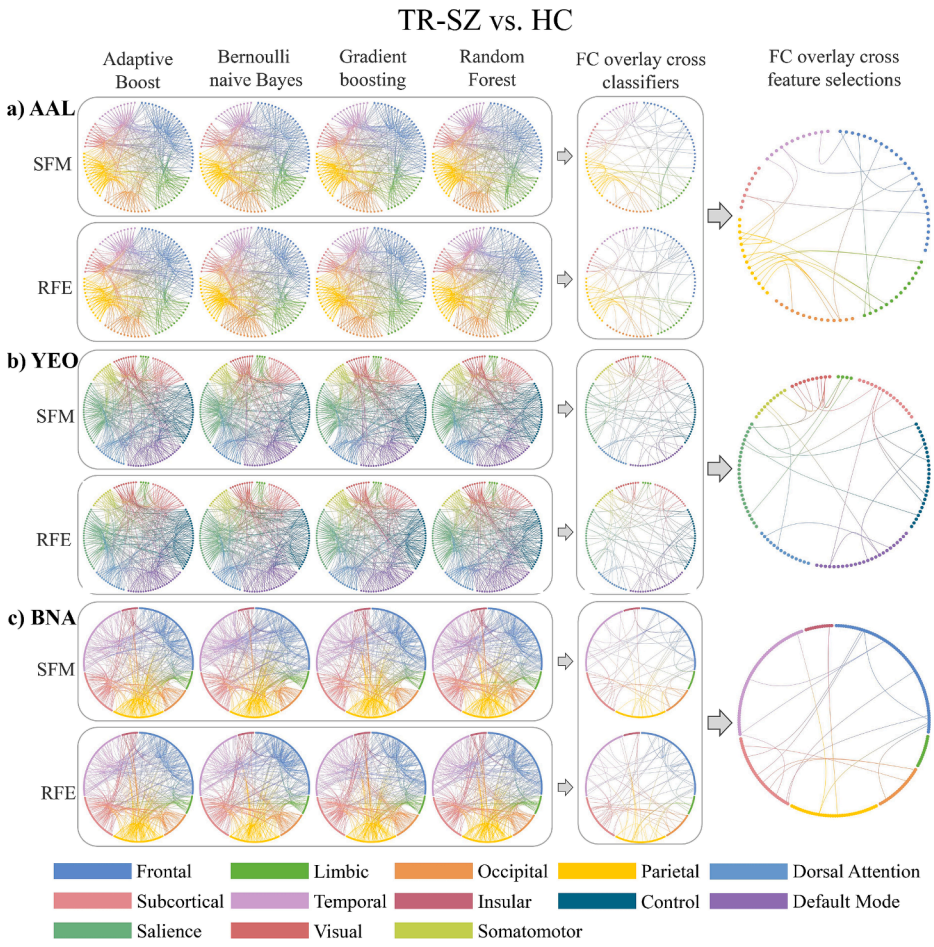

Fig. 2. The top 40% contributed FCs from AAL (a), YEO (b) and BNA (c) atlases in distinguishing TR-SZ and HC. Abbreviations (alphabetical order): AAL: automated anatomical labeling, BNA: Brainnetome, FC: Functional connection, HC: healthy control, RFE: Recursive Feature Elimination, SFM: Select From Model, TR-SZ: treatment-resistant schizophrenia, YEO: Yeo-Networks.

parahippocampal gyrus/basal ganglia, lateral occipital cortex-basal ganglia/superior parietal lobule, cingulate gyrus-middle frontal gyrus/fusiform gyrus, precuneus-orbital gyrus/medial occipital cortex, paracentral lobule-inferior parietal lobule, postcentral gyrus-thalamus were the consistent for BNA (Fig. 3**c**). Details on the consistent FCs over AAL, YEO and BNA in discriminating NTR-SZ and HC are given in Supplementary Table 6. Comparing AAL, YEO and BNA, the frontal-limbic, frontal-parietal, frontal-temporal, limbic-parietal, limbic-occipital and limbic-temporal FCs were consistent in distinguish NTR-SZ and HC.

4.4. Consistent FCs in distinguish TR-SZ and NTR-SZ

The FCs between superior frontal gyrus-insula, lingual gyrus-postcentral gyrus, cuneus-inferior parietal gyrus, precuneus-angular gyrus, inferior frontal gyrus-supramarginal gyrus, olfactory cortex-pallidum/thalamus, inferior occipital gyrus-pallidum, lingual gyrus-middle temporal gyrus were the consistent for AAL (Fig. 4**a**). The FCs between ventral attention network-default mode network/somatomotor/visual network/control network/subcortex, subcortex-visual network/subcortex were the consistent for YEO (Fig. 4**b**). The FCs between middle temporal gyrus-inferior temporal gyrus/hippocampus/basal ganglia, medial occipital cortex-middle frontal gyrus/superior temporal sulcus/parahippocampal gyrus, inferior parietal lobule-orbital gyrus/cingulate gyrus, thalamus-inferior temporal gyrus/basal ganglia, amygdala-superior frontal gyrus were the consistent for BNA (Fig. 4**c**). Details on the consistent FCs over AAL, YEO and BNA in distinguishing TR-SZ and NTR-SZ can be found in Supplementary Table 7. Comparing AAL, YEO and BNA, the frontal-limbic, frontal-parietal and occipital-temporal FCs were consistent in distinguish TR-SZ and NTR-SZ.

4.5. Consistent frontal-limbic FCs in all the diagnosis of SZ

The frontal-limbic and frontal-parietal connectivity were consistently found in all the SZ diagnosis (TR-SZ vs. HC, NTR-SZ vs. HC, TR-SZ vs. NTR-SZ), in which the frontal-limbic, frontal-parietal and occipital-temporal FCs were consistent in differentiating TR-SZ and NTR-SZ (Fig. 5**a**). All the above consistent FCs overlaid with 3 atlases were not correlated with age, gender and education. The BNA atlas achieved the highest classification accuracy (>90%) compared with AAL and YEO in all the diagnosis tasks (TR-SZ vs. HC, NTR-SZ vs. HC and TR-SZ vs. NTR-SZ, Fig. 5**c**).

The identified consistent frontal-limbic, frontal-parietal and occipital-temporal FCs in distinguishing TR-SZ and NTR-SZ were found to be correlated with disease progression (disease duration), symptoms (PANSS negative) and medication dosage (OLA-ED, Fig. 5**b**, Supplementary Table 8). Specifically, in TR-SZ and NTR-SZ (together): four FCs between middle temporal gyrus (MTG)-lingual gyrus (LING), precuneus (PCUN)-inferior parietal lobule (IPL), and putamen (PUT)-nucleus accumbens (NAc) were associated with disease duration ($r = 0.15$, $p_{uncorrected} = 0.0081$; $r = 0.20$, $p_{uncorrected} = 0.00061$; $r = 0.15$, $p_{uncorrected} = 0.0080$), respectively; the PCUN-IPL FC was correlated with OLA-ED ($r = 0.15$, $p_{uncorrected} = 0.0081$); the pallidum (PAL)-olfactory cortex (OLF) FC was associated with PANSS negative ($r = 0.16$, $p_{uncorrected} = 0.0072$). Among these, the FC between PCUN-IPL, which

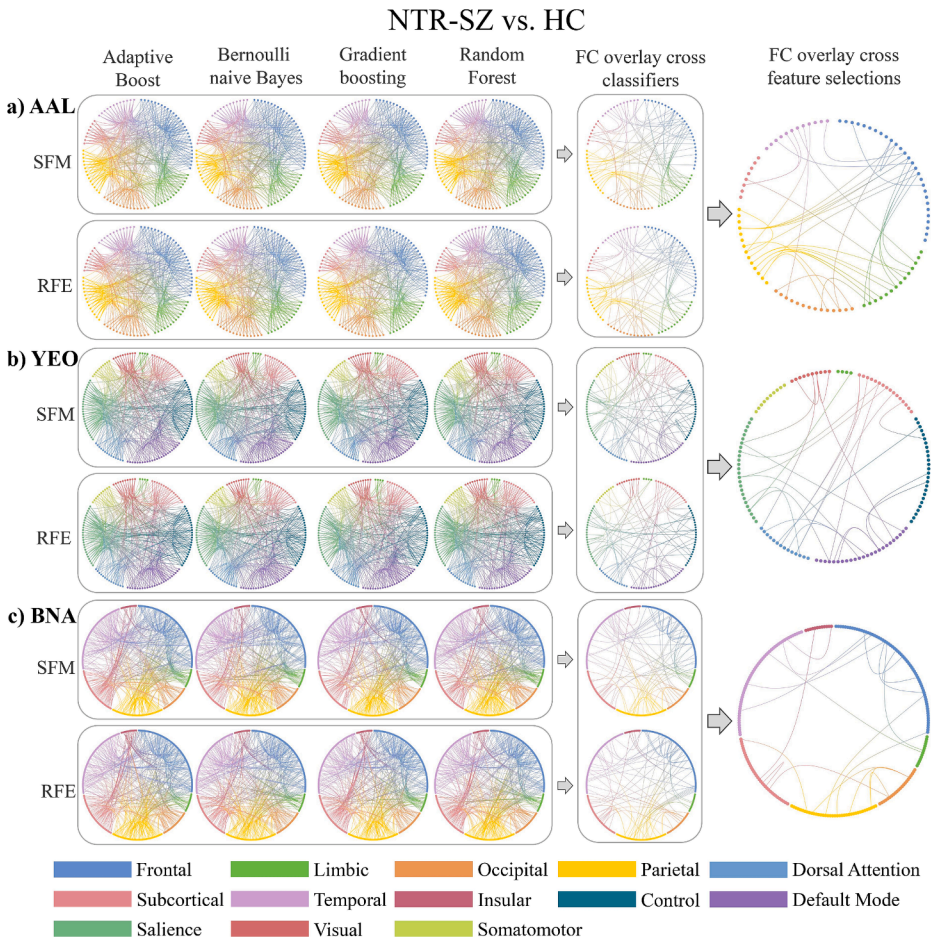

Fig. 3. The top 40% contributed FCs from AAL (a), YEO (b) and BNA (c) atlases in distinguishing NTR-SZ and HC. Abbreviations (alphabetical order): AAL: automated anatomical labeling, BNA: Brainnetome, FC: Functional connection, HC: healthy control, NTR-SZ: non-treatment-resistant schizophrenia, RFE: Recursive Feature Elimination, SFM: Select From Model, YEO: Yeo-Networks.

was associated with disease duration, passed the Bonferroni correction ($p_{corrected} = 0.014$).

5. Discussion

This study investigated the differences among TR-SZ, NTR-SZ and HC using 3 atlases, 2 feature selections and 4 classifiers to identify the consistent FCs. As summarized in Fig. 5, this study demonstrated the following results. (1) The whole brain FCs, except the temporal-occipital FC, were consistent in distinguishing SZ and HCs (TR-SZ vs. HC and NTR-SZ vs. HC). (2) Abnormal frontal-limbic, frontal-parietal and occipital-temporal FCs were consistent over 3 atlases, 2 feature selections and 4 classifiers in distinguishing TR-SZ and NTR-SZ. (3) The consistent frontal-limbic, frontal-parietal and occipital-temporal FCs were further correlated with disease progression, symptoms and medication dosage. (4) The frontal-limbic and frontal-parietal FCs were highly consistent for the diagnosis of SZ across 3 atlases. (5) The BNA atlas achieved the highest classification accuracy (>90%) comparing with AAL and YEO in most diagnosis tasks (TR-SZ vs. HC, NTR-SZ vs. HC and TR-SZ vs. NTR-SZ).

The whole brain FCs, except the temporal-occipital FC, reflect the differences between SZ (TR-SZ/NTR-SZ) and HC robustly. Consistent with our results, a previous study reported that abnormal FCs were widely distributed in the whole brain in the diagnosis of SZ (Hua et al., 2020). Similarly, both data-driven and seed-based analyses identified elevated global brain signal variability in SZ (Yang et al., 2014). Decreased FCs between temporal cortex-amygdala and putamen-temporal/postcentral cortex were observed in distinguishing SZ between HC (Erdeniz et al., 2017). SZ also exhibited decreased FCs in precuneus, frontal, temporal, cerebellum and cingulate cortex when the hippocampus served as seed regions (Duan et al., 2015). Lower FCs between 14 distinct cerebellar network pairs were identified in first-episode SZ (Feng et al., 2022). Widespread dynamic FCs involving sensorimotor, attention, limbic and subcortical areas at both regional and network levels (Long et al., 2020) were found in SZ. These results showed that SZ influences the strength and efficiency of connections between almost all the brain regions, indicating that SZ may involve brain network abnormalities across multiple levels.

The frontal-limbic, frontal-parietal and occipital-temporal neural circuits are the identified consistent FCs in differentiating TR-SZ and NTR-SZ. Previously cortical surface modelling identified decreased cortical thickness in prefrontal cortex between TR-SZ and NTR-SZ (Zugman et al., 2013). Statistical analysis of cortical volume and thickness in TR-SZ showed significant reductions in frontal, parietal, occipital, temporal and cingulate cortex comparing with NTR-SZ (Barry et al., 2019). Direct group comparisons between TR-SZ and NTR-SZ found reduced cortical thickness in frontal, fusiform gyrus (namely the medial occipitotemporal gyrus) and Supramarginal cortex, a part of parietal (Fan et al., 2023). Furthermore, TR-SZ exhibited reduced FC within limbic between ventral striatum and substantia nigra compared to NTR-SZ (White et al., 2016). Regional homogeneity revealed widespread discrepancy in frontal and fusiform gyrus between TR-SZ and NTR-SZ (Gao et al., 2018). Comparing with the whole brain FCs (except the occipital-temporal) in distinguishing SZ and HC, the occipital-

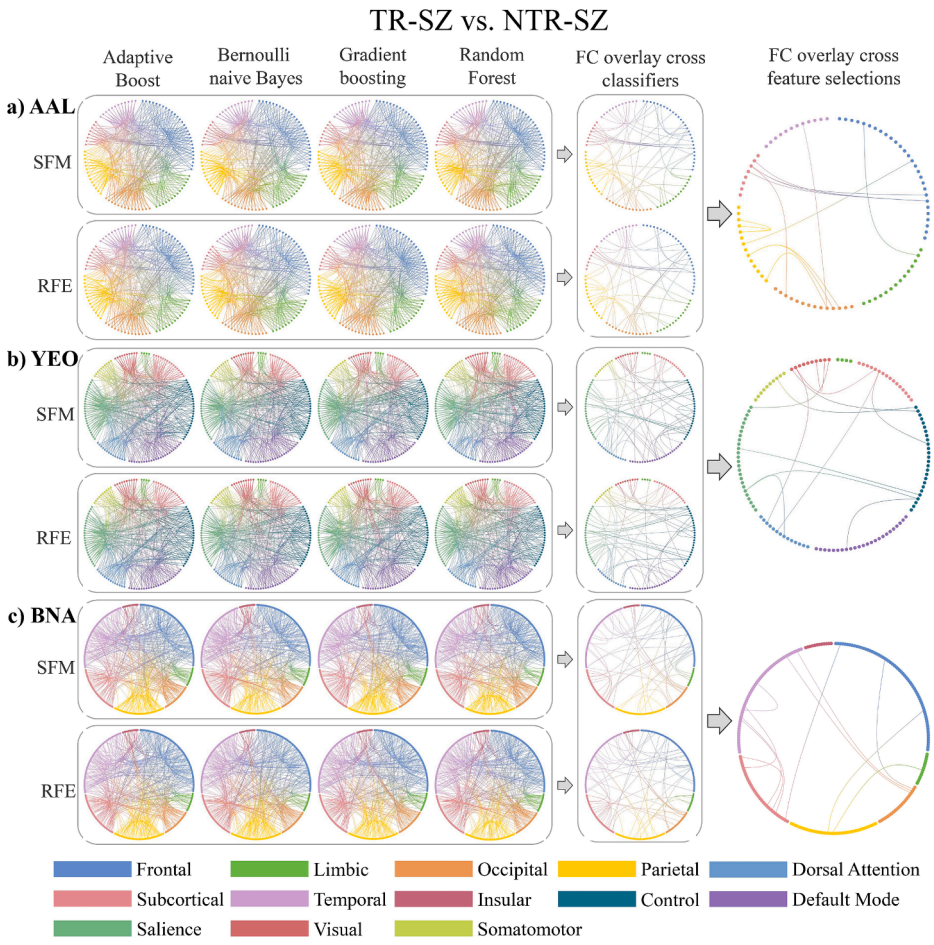

Fig. 4. The top 40% contributed FCs from AAL (a), YEO (b) and BNA (c) atlases in distinguishing TR-SZ and NTR-SZ. Abbreviations (alphabetical order): AAL: automated anatomical labeling, BNA: Brainnetome, FC: Functional connection, NTR-SZ: non-treatment-resistant schizophrenia, RFE: Recursive Feature Elimination, SFM: Select From Model, TR-SZ: treatment-resistant schizophrenia, YEO: Yeo-Networks.

temporal FC is specific in distinguishing TR-SZ and NTR-SZ. This indicate that the occipital- temporal FC may be a potential target in recognizing those TR-SZ in the clinical practice. The consistent frontal-limbic, frontal-parietal and occipital-temporal FCs in differentiating TR-SZ and NTR-SZ were further correlated with disease progression, symptoms and medication dosage, providing valuable preliminary insights into the interaction between medication/symptoms and FCs.

Frontal-limbic neural circuit is associated with affective and psychotic symptoms of schizophrenia. Moreover, the frontal-parietal network, which plays a pivotal role in the human brain, is linked to the disorganization symptoms observed in schizophrenia (Rotarska-Jagiela et al., 2010). In differentiating SZ from HC, we observed a high degree of consistency in the frontal-limbic and frontal-parietal FCs across all the 3 diagnosis tasks. Reduced FC between posterior cingulate cortex and frontal cortex (Liang et al., 2020) with increased FC between frontal cortex and putamen were identified in SZ. Similarly, decreased FC in amygdala-frontal cortex was found in first-episode SZ (Wang et al., 2020). SZ also exhibited reduced FC in the frontal cortex-hippocampus comparing with HC (Wang et al., 2021). For the prefrontal-parietal network, abnormalities in the SZ can result in functional impairments, including those related to retrieval, storage, and maintenance (Mwansisya et al., 2017). Compared to HC, SZ exhibited decreased positive FC between frontal to parietal network (Chahine et al., 2017; Wu et al., 2017). Consistent with these findings, abnormal frontal-limbic and frontal-parietal neural pathways are highly consistent in SZ, and may serve as a potential diagnostic biomarker with future clinical application. Furthermore, the BNA (which involves the most brain areas) outperformed AAL and YEO across the 3 diagnosis tasks, with better classification accuracy.

One possible limitation is that all SZ patients were treated with antipsychotic medications and these drugs are known to affect structural and functional brain measures (Pereira-Sanchez et al., 2021). Hence, FC differences between SZ and HC may be confounded by antipsychotic exposure. Similarly, the differences between TR-SZ and NTR-SZ could be accounted by higher OLA-ED exposure in the former group. Another limitation is the lack of external dataset validation. There is no additional data on TR-SZ and NTR-SZ to support validation, resulting in the absence of further validation of the conclusions obtained. However, 3 atlases, 2 feature selections and 4 classifiers were employed to identify the most consistent findings for each diagnostic task, demonstration the results being robust to method variation. Additionally, all participants were recruited from one single site, which may introduce site-specific biases and limit the generalizability of the findings. The TR-SZ group also had a longer duration of illness on average, which could have influenced the results. Finally, the number of subjects in the different categories was unbalanced. However, the data was randomly subsampled 1000 times to ensure the balance of the data before the classification.

In conclusion, to the best of our knowledge, this is the first attempt to investigate the robust FCs in distinguishing TR-SZ and NTR-SZ over 3 atlases, with 2 feature selections and 4 classifiers. Whole brain FCs, except the temporal-occipital FC, were consistent in distinguishing SZ and HC. While, abnormal frontal-limbic, frontal-parietal and occipital-temporal FCs were consistent over three atlases in distinguishing TR-

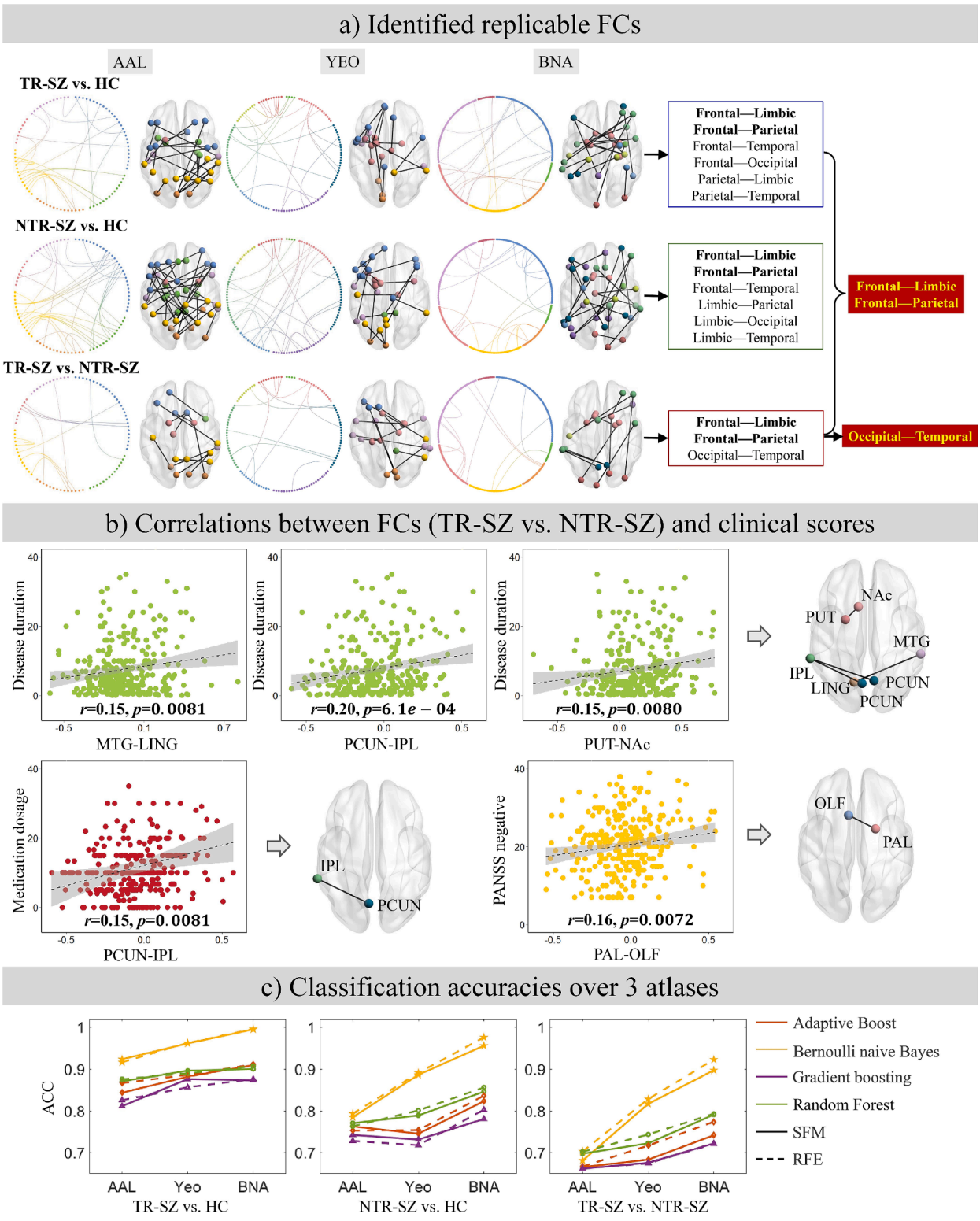

Fig. 5. (a) Frontal-limbic and frontal-parietal FCs were highly consistent in all the SZ diagnosis (TR-SZ vs. HC, NTR-SZ vs. HC, TR-SZ vs. NTR-SZ). (b) Consistent frontal-limbic, frontal-parietal and occipital-temporal FCs were correlated with the disease duration, PANSS negative and OLA-ED. (c) Classification accuracy comparisons over the three atlases under 2 feature selections, and 4 classifiers. Abbreviations (alphabetical order): AAL: automated anatomical labeling, ACC: accuracy, BNA: Brainnetome, FC: functional connection, HC: healthy control, IPL: inferior parietal lobule, LING: lingual gyrus, MTG: middle temporal gyrus, NAc: Nucleus accumbens, NTR-SZ: non-treatment-resistant schizophrenia, OLA-ED: equivalent doses of olanzapine, OLF: olfactory cortex, PAL: pallidum, PCUN: precuneus, PUT: putamen, RFE: Recursive Feature Elimination, SFM: Select From Model, TR-SZ: treatment-resistant schizophrenia, YEO: Yeo-Networks.

SZ and NTR-SZ, that were further correlated with disease progression, symptoms and medication dosage. These results indicate that the frontal-limbic and frontal-parietal FCs are robust neural pathways in the diagnosis of SZ, whereas the frontal-limbic, frontal-parietal and occipital-temporal FCs are informative in recognizing those TR-SZ in the clinical practice. For example, a simple 5–10 min resting fMRI scan has the potential to assist in identifying whether a SZ patient may benefit from alternative treatment strategies, such as clozapine, for treatment-resistant psychosis. However, further prospective studies are required to establish the prognostic utility of rs-fMRI classifiers.

Author contributions

Yijie Zhang performed the data analysis and wrote the initial draft. Shuzhan Gao wrote the manuscript. Shile Qi and Xijia Xu conceptualized the study. Chuang liang, Juan Bustillo, Peter Kochunov, Jessica A. Turner, Vince D. Calhoun, Rongtao Jiang, Daoqiang Zhang, Jing Jiang, Fan Wu and Ting Peng revised the manuscript. Zening Fu and Lei Wu preprocessed the MRI data.

CRediT authorship contribution statement

Yijie Zhang: Writing – original draft, Visualization, Validation, Methodology, Formal analysis. **Shuzhan Gao:** Writing – original draft. **Chuang Liang:** Writing – review & editing. **Juan Bustillo:** Writing – review & editing. **Peter Kochunov:** Writing – review & editing. **Jessica A. Turner:** Writing – review & editing. **Vince D. Calhoun:** Writing – review & editing. **Lei Wu:** Data curation. **Zening Fu:** Data curation. **Rongtao Jiang:** Writing – review & editing. **Daoqiang Zhang:** Writing – review & editing. **Jing Jiang:** Writing – review & editing. **Fan Wu:** Writing – review & editing. **Ting Peng:** Writing – review & editing. **Xijia Xu:** Conceptualization. **Shile Qi:** Conceptualization.

Declaration of Competing Interest

The authors declare that they have no known competing financial interests or personal relationships that could have appeared to influence the work reported in this paper.

Acknowledgements

This work was supported by grants from the Key Research and Development Plan in Jiangsu (Social Development), China (BE2022677, BE2023668), the National Natural Science Foundation of China (62376124, 82172061, 81771444 and 82371510), the Natural Science Foundation of Jiangsu Province, China (BK20220889), the Fundamental Research Funds for the Central Universities (NJ2023032) and the National Key Research and Development Program of China (2023YFF1204803).

Appendix A. Supplementary data

Supplementary data to this article can be found online at https://doi.org/10.1016/j.nicl.2024.103726.

Data availability

The authors do not have permission to share data.

References

Aggarwal, A., Grover, S., Ahuja, C., Chakrabarti, S., Khandelwal, N., Avasthi, A., 2021. A comparative diffusion tensor imaging study of patients with and without treatment-resistant schizophrenia. Indian J. Psychiatry 63, 146–151.
Bae, Y., Kumarasamy, K., Ali, I.M., Korfiatis, P., Akkus, Z., Erickson, B.J., 2018. Differences between schizophrenic and normal subjects using network properties from fMRI. J. Digit. Imaging 31, 252–261.
Barry, E.F., Vanes, L.D., Andrews, D.S., Patel, K., Horne, C.M., Mouchlianitis, E., Hellyer, P.J., Shergill, S.S., 2019. Mapping cortical surface features in treatment resistant schizophrenia with in vivo structural MRI. Psychiatry Res. 274, 335–344.
Breiman, L., 2001. Random forests. Machine Learn. 45, 5–32.
Canario, E., Chen, D., Biswal, B., 2021. A review of resting-state fMRI and its use to examine psychiatric disorders. Psychoradiology 1, 42–53.
Chahine, G., Richter, A., Wolter, S., Goya-Maldonado, R., Gruber, O., 2017. Disruptions in the left frontoparietal network underlie resting state endophenotypic markers in schizophrenia. Hum Brain Mapp 38, 1741–1750.
Correll, C.U., Agid, O., Crespo-Facorro, B., De Bartolomeis, A., Fagiolini, A., Seppälä, N., Howes, O.D., 2022. A guideline and checklist for initiating and managing clozapine treatment in patients with treatment-resistant schizophrenia. CNS Drugs 36, 659–679.
Crespo-Facorro, B., de la Foz, V.-O.-G., Ayesa-Arriola, R., Pérez-Iglesias, R., Mata, I., Suarez-Pinilla, P., Tabares-Seisdedos, R., Vázquez-Barquero, J.L., 2013. Prediction of acute clinical response following a first episode of non affective psychosis: results of a cohort of 375 patients from the Spanish PAFIP study. Prog. Neuropsychopharmacol. Biol. Psychiatry 44, 162–167.
Dai, B., Ding, S., Wahba, G., 2013. Multivariate Bernoulli distribution. Bernoulli 19 (1465–1483), 1419.
Duan, H.-F., Gan, J.-L., Yang, J.-M., Cheng, Z.-X., Gao, C.-Y., Shi, Z.-J., Zhu, X.-Q., Liang, X.-J., Zhao, L.-M., 2015. A longitudinal study on intrinsic connectivity of hippocampus associated with positive symptom in first-episode schizophrenia. Behav. Brain Res. 283, 78–86.
Elliott, M.L., Knodt, A.R., Hariri, A.R., 2021. Striving toward translation: strategies for reliable fMRI measurement. Trends Cogn. Sci. 25, 776–787.
Erdeniz, B., Serin, E., İbadi, Y., Taş, C., 2017. Decreased functional connectivity in schizophrenia: The relationship between social functioning, social cognition and graph theoretical network measures. Psychiatry Res. Neuroimaging 270, 22–31.
Fan, F., Huang, J., Tan, S., Wang, Z., Li, Y., Chen, S., Li, H., Hare, S., Du, X., Yang, F., Tian, B., Kochunov, P., Tan, Y., Hong, L.E., 2023. Association of cortical thickness and cognition with schizophrenia treatment resistance. Psychiatry Clin. Neurosci. 77, 12–19.
Fan, L., Li, H., Zhuo, J., Zhang, Y., Wang, J., Chen, L., Yang, Z., Chu, C., Xie, S., Laird, A. R., Fox, P.T., Eickhoff, S.B., Yu, C., Jiang, T., 2016. The human brainnetome Atlas: a new brain atlas based on connectional architecture. Cereb. Cortex 26, 3508–3526.
Feng, S., Zheng, S., Zou, H., Dong, L., Zhu, H., Liu, S., Wang, D., Ning, Y., Jia, H., 2022. Altered functional connectivity of cerebellar networks in first-episode schizophrenia. Front. Cell. Neurosci. 16.
Finn, E.S., Poldrack, R.A., Shine, J.M., 2023. Functional neuroimaging as a catalyst for integrated neuroscience. Nature 623, 263–273.
Ganella, E.P., Bartholomeusz, C.F., Seguin, C., Whittle, S., Bousman, C., Phassouliotis, C., Everall, I., Pantelis, C., Zalesky, A., 2017. Functional brain networks in treatment-resistant schizophrenia. Schizophr. Res. 184, 73–81.
Gao, S., Lu, S., Shi, X., Ming, Y., Xiao, C., Sun, J., Yao, H., Xu, X., 2018. Distinguishing between treatment-resistant and non-treatment-resistant schizophrenia using regional homogeneity. Front. Psych. 9, 282.
Hasan, A., Falkai, P., Wobrock, T., Lieberman, J., Glenthoj, B., Gattaz, W.F., Thibaut, F., Möller, H.-J., Schizophrenia, W.T.F.o.T.G.f., 2012. World Federation of Societies of Biological Psychiatry (WFSBP) Guidelines for Biological Treatment of Schizophrenia, part 1: update 2012 on the acute treatment of schizophrenia and the management of treatment resistance. World J. Biol. Psychiatry 13, 318–378.
Howes, O.D., McCutcheon, R., Agid, O., De Bartolomeis, A., Van Beveren, N.J., Birnbaum, M.L., Bloomfield, M.A., Bressan, R.A., Buchanan, R.W., Carpenter, W.T., 2017. Treatment-resistant schizophrenia: treatment response and resistance in psychosis (TRRIP) working group consensus guidelines on diagnosis and terminology. Am. J. Psychiatry 174, 216–229.
Hua, M., Peng, Y., Zhou, Y., Qin, W., Yu, C., Liang, M., 2020. Disrupted pathways from limbic areas to thalamus in schizophrenia highlighted by whole-brain resting-state effective connectivity analysis. Prog. Neuropsychopharmacol. Biol. Psychiatry 99, 109837.
Itahashi, T., Noda, Y., Iwata, Y., Tarumi, R., Tsugawa, S., Plitman, E., Honda, S., Caravaggio, F., Kim, J., Matsushita, K., Gerretsen, P., Uchida, H., Remington, G., Mimura, M., Aoki, Y.Y., Graff-Guerrero, A., Nakajima, S., 2021. Dimensional distribution of cortical abnormality across antipsychotics treatment-resistant and responsive schizophrenia. NeuroImage: Clinical 32, 102852.
Kay, S.R., Fiszbein, A., Opler, L.A., 1987. The positive and negative syndrome scale (PANSS) for schizophrenia. Schizophr. Bull. 13, 261–276.
Kim, W.S., Shen, J., Tsogt, U., Odkhuu, S., Chung, Y.C., 2022. Altered thalamic subregion functional networks in patients with treatment-resistant schizophrenia. World J. Psychiatry 12, 693–707.
Leucht, S., Samara, M., Heres, S., Davis, J.M., 2016. Dose equivalents for antipsychotic drugs: the DDD method. Schizophr. Bull. 42, S90–S94.
Liang, S., Deng, W., Li, X., Wang, Q., Greenshaw, A.J., Guo, W., Kong, X., Li, M., Zhao, L., Meng, Y., Zhang, C., Yu, H., Li, X.-M., Ma, X., Li, T., 2020. Aberrant posterior cingulate connectivity classify first-episode schizophrenia from controls: a machine learning study. Schizophr. Res. 220, 187–193.
Liang, C., Pearlson, G., Bustillo, J., Kochunov, P., Turner, J.A., Wen, X., Jiang, R., Fu, Z., Zhang, X., Li, K., 2023. Psychotic symptom, mood, and cognition-associated multimodal MRI reveal shared links to the salience network within the psychosis spectrum disorders. Schizophr. Bull. 49, 172–184.
Long, Y., Liu, Z., Chan, C.K.Y., Wu, G., Xue, Z., Pan, Y., Chen, X., Huang, X., Li, D., Pu, W., 2020. Altered temporal variability of local and large-scale resting-state brain functional connectivity patterns in schizophrenia and bipolar disorder. Front. Psychiatry 11.

Matrone, M., Kotzalidis, G.D., Romano, A., Bozzao, A., Cuomo, I., Valente, F., Gabaglio, C., Lombardozzi, G., Trovini, G., Amici, E., Perrini, F., De Persis, S., Iasevoli, F., De Filippis, S., de Bartolomeis, A., 2022. Treatment-resistant schizophrenia: Addressing white matter integrity, intracortical glutamate levels, clinical and cognitive profiles between early- and adult-onset patients. Prog. Neuropsychopharmacol. Biol. Psychiatry 114, 110493.

McNabb, C.B., Tait, R.J., McIlwain, M.E., Anderson, V.M., Suckling, J., Kydd, R.R., Russell, B.R., 2018. Functional network dysconnectivity as a biomarker of treatment resistance in schizophrenia. Schizophr. Res. 195, 160–167.

McNabb, C.B., McIlwain, M.E., Anderson, V.M., Kydd, R.R., Sundram, F., Russell, B.R., 2020. Aberrant white matter microstructure in treatment-resistant schizophrenia. Psychiatry Res. Neuroimaging 305, 111198.

Moghimi, P., Dang, A.T., Do, Q., Netoff, T.I., Lim, K.O., Atluri, G., 2022. Evaluation of functional MRI-based human brain parcellation: a review. J Neurophysiol 128, 197–217.

Mwansisya, T.E., Hu, A., Li, Y., Chen, X., Wu, G., Huang, X., Lv, D., Li, Z., Liu, C., Xue, Z., 2017. Task and resting-state fMRI studies in first-episode schizophrenia: a systematic review. Schizophr. Res. 189, 9–18.

Natekin, A., Knoll, A., 2013. Gradient boosting machines, a tutorial. Front. Neurorob. 7, 21.

Nucifora Jr, F.C., Woznica, E., Lee, B.J., Cascella, N., Sawa, A., 2019. Treatment resistant schizophrenia: clinical, biological, and therapeutic perspectives. Neurobiol. Dis. 131, 104257.

Ochi, R., Noda, Y., Tsuchimoto, S., Tarumi, R., Honda, S., Matsushita, K., Tsugawa, S., Plitman, E., Masuda, F., Ogyu, K., Wada, M., Miyazaki, T., Fujii, S., Chakravarty, M. M., Graff-Guerrero, A., Uchida, H., Mimura, M., Nakajima, S., 2020. White matter microstructural organizations in patients with severe treatment-resistant schizophrenia: a diffusion tensor imaging study. Prog. Neuropsychopharmacol. Biol. Psychiatry 100, 109871.

Orban, P., Dansereau, C., Desbois, L., Mongeau-Pérusse, V., Giguère, C.-É., Nguyen, H., Mendrek, A., Stip, E., Bellec, P., 2018. Multisite generalizability of schizophrenia diagnosis classification based on functional brain connectivity. Schizophr. Res. 192, 167–171.

Pereira-Sanchez, V., Franco, A.R., Vieira, D., de Castro-Manglano, P., Soutullo, C., Milham, M.P., Castellanos, F.X., 2021. Systematic review: medication effects on brain intrinsic functional connectivity in patients with attention-deficit/hyperactivity disorder. J. Am. Acad. Child Adolesc. Psychiatry 60, 222–235.

Qi, S., Bustillo, J., Turner, J.A., Jiang, R., Zhi, D., Fu, Z., Deramus, T.P., Vergara, V., Ma, X., Yang, X., Stevens, M., Zhuo, C., Xu, Y., Calhoun, V.D., Sui, J., 2020. The relevance of transdiagnostic shared networks to the severity of symptoms and cognitive deficits in schizophrenia: a multimodal brain imaging fusion study. Transl. Psychiatry 10, 149.

Qi, S., Sui, J., Pearlson, G., Bustillo, J., Perrone-Bizzozero, N.I., Kochunov, P., Turner, J. A., Fu, Z., Shao, W., Jiang, R., Yang, X., Liu, J., Du, Y., Chen, J., Zhang, D., Calhoun, V.D., 2022. Derivation and utility of schizophrenia polygenic risk associated multimodal MRI frontotemporal network. Nat. Commun. 13, 4929.

Qureshi, M.N.I., Oh, J., Lee, B., 2019. 3D-CNN based discrimination of schizophrenia using resting-state fMRI. Artif. Intell. Med. 98, 10–17.

Rish, I., 2001. An empirical study of the naive Bayes classifier. IJCAI 2001 workshop on empirical methods in artificial intelligence, pp. 41–46.

Rotarska-Jagiela, A., van de Ven, V., Oertel-Knöchel, V., Uhlhaas, P.J., Vogeley, K., Linden, D.E., 2010. Resting-state functional network correlates of psychotic symptoms in schizophrenia. Schizophr. Res. 117, 21–30.

Schapire, R.E., 2013. Explaining AdaBoost. Springer, Berlin Heidelberg, pp. 37–52.

Shah, P., Plitman, E., Iwata, Y., Kim, J., Nakajima, S., Chan, N., Brown, E.E., Caravaggio, F., Torres, E., Hahn, M., 2020. Glutamatergic neurometabolites and cortical thickness in treatment-resistant schizophrenia: implications for glutamate-mediated excitotoxicity. J. Psychiatr. Res. 124, 151–158.

Shi, D., Li, Y., Zhang, H., Yao, X., Wang, S., Wang, G., Ren, K., 2021. Machine learning of schizophrenia detection with structural and functional neuroimaging. Dis. Markers 2021, 9963824.

Shin, S., Jung, W.H., McCutcheon, R., Veronese, M., Beck, K., Lee, J.S., Lee, Y.-S., Howes, O.D., Kim, E., Kwon, J.S., 2022. The relationship between frontostriatal connectivity and striatal dopamine function in schizophrenia: an 18F-DOPA PET and diffusion tensor imaging study in treatment responsive and resistant patients. Psychiatry Investig. 19, 570–579.

Siskind, D., Orr, S., Sinha, S., Yu, O., Brijball, B., Warren, N., Maccabe, J.H., Smart, S.E., Kisely, S., 2022. Rates of treatment-resistant schizophrenia from first-episode cohorts: systematic review and meta-analysis. Br. J. Psychiatry 220, 115–120.

Su, L., Wang, L., Shen, H., Feng, G., Hu, D., 2013. Discriminative analysis of non-linear brain connectivity in schizophrenia: an fMRI Study. Front. Hum. Neurosci. 7, 702.

Tian, Y., Margulies, D.S., Breakspear, M., Zalesky, A., 2020. Topographic organization of the human subcortex unveiled with functional connectivity gradients. Nat. Neurosci. 23, 1421–1432.

Tzourio-mazoyer, N., Landeau, B., Papathanassiou, D., Crivello, F., Etard, O., Delcroix, N., Mazoyer, B., Joliot, M., 2002. Automated anatomical labeling of activations in SPM using a macroscopic anatomical parcellation of the MNI MRI single-subject brain. Neuroimage 15, 273–289.

Wang, G., Lyu, H., Wu, R., Ou, J., Zhu, F., Liu, Y., Zhao, J., Guo, W., 2020. Resting-state functional hypoconnectivity of amygdala in clinical high risk state and first-episode schizophrenia. Brain Imaging Behav. 14, 1840–1849.

Wang, X., Yin, Z., Sun, Q., Jiang, X., Chao, L., Dai, X., Tang, Y., 2021. Comparative study on the functional connectivity of amygdala and hippocampal neural circuits in patients with first-episode schizophrenia and other high-risk populations. Front. Psych. 12, 627198.

Wannan, C.M.J., Cropley, V.L., Chakravarty, M.M., Bousman, C., Ganella, E.P., Bruggemann, J.M., Weickert, T.W., Weickert, C.S., Everall, I., McGorry, P., Velakoulis, D., Wood, S.J., Bartholomeusz, C.F., Pantelis, C., Zalesky, A., 2019. Evidence for network-based cortical thickness reductions in schizophrenia. Am. J. Psychiatry 176, 552–563.

White, T.P., Wigton, R., Joyce, D.W., Collier, T., Fornito, A., Shergill, S.S., 2016. Dysfunctional striatal systems in treatment-resistant schizophrenia. Neuropsychopharmacology 41, 1274–1285.

Who, 1992. The ICD-10 Classification of Mental and Behavioural Disorders: Clinical Descriptions and Diagnostic Guidelines. World Health Organization.

Winterburn, J.L., Voineskos, A.N., Devenyi, G.A., Plitman, E., de la Fuente-Sandoval, C., Bhagwat, N., Graff-Guerrero, A., Knight, J., Chakravarty, M.M., 2019. Can we accurately classify schizophrenia patients from healthy controls using magnetic resonance imaging and machine learning? A multi-method and multi-dataset study. Schizophr. Res. 214, 3–10.

Wu, X.-J., Zeng, L.-L., Shen, H., Yuan, L., Qin, J., Zhang, P., Hu, D., 2017. Functional network connectivity alterations in schizophrenia and depression. Psychiatry Res. Neuroimaging 263, 113–120.

Yan, W., Calhoun, V., Song, M., Cui, Y., Yan, H., Liu, S., Fan, L., Zuo, N., Yang, Z., Xu, K., 2019. Discriminating schizophrenia using recurrent neural network applied on time courses of multi-site FMRI data. EBioMedicine 47, 543–552.

Yang, G.J., Murray, J.D., Repovs, G., Cole, M.W., Savic, A., Glasser, M.F., Pittenger, C., Krystal, J.H., Wang, X.-J., Pearlson, G.D., Glahn, D.C., Anticevic, A., 2014. Altered global brain signal in schizophrenia. Proc. Natl. Acad. Sci. 111, 7438–7443.

Yeo, B.T., Krienen, F.M., Sepulcre, J., Sabuncu, M.R., Lashkari, D., Hollinshead, M., Roffman, J.L., Smoller, J.W., Zöllei, L., Polimeni, J.R., 2011. The organization of the human cerebral cortex estimated by intrinsic functional connectivity. J. Neurophysiol.

Zhao, C., Jiang, R., Bustillo, J., Kochunov, P., Turner, J.A., Liang, C., Fu, Z., Zhang, D., Qi, S., Calhoun, V.D., 2024. Cross-cohort replicable resting-state functional connectivity in predicting symptoms and cognition of schizophrenia. Hum. Brain Mapp. 45, e26694.

Zugman, A., Gadelha, A., Assunção, I., Sato, J., Ota, V.K., Rocha, D.L., Mari, J.J., Belangero, S.I., Bressan, R.A., Brietzke, E., Jackowski, A.P., 2013. Reduced dorso-lateral prefrontal cortex in treatment resistant schizophrenia. Schizophr. Res. 148, 81–86.